

Reactions of imido complexes of iridium, rhodium and ruthenium

Andreas A. Danopoulos,^a Geoffrey Wilkinson,^{*a} Tracy K. N. Sweet^b and Michael B. Hursthouse^{*b}^a Johnson Matthey Laboratory, Chemistry Department, Imperial College, London SW7 2AY, UK^b Department of Chemistry, University of Wales Cardiff, PO Box 912, Cardiff CF1 3TB, UK

Interactions of the known compounds $\text{Ir}(\eta\text{-C}_5\text{Me}_5)(\text{NR})$ ($\text{R} = \text{Bu}^1$ **1a** or 2,6- $\text{Pr}^i_2\text{C}_6\text{H}_3$ **1b**) with 2,6-xylyl isocyanide $[(\text{xyl})\text{NC}]$, mesityl isocyanate and mesityl azide (mesityl = mes = $\text{C}_6\text{H}_2\text{Me}_3$ -2,4,6) have been studied. The bridged dimers $[\text{Ir}(\eta\text{-C}_5\text{Me}_5)(\mu\text{-NC}_5\text{H}_9)]_2$ **2** and $[\text{Ir}_2(\eta\text{-C}_5\text{Me}_5)_2(\mu\text{-NC}_6\text{H}_{11})(\mu\text{-NHC}_6\text{H}_{11})]\text{Cl}$ **3** have been synthesized. Reactions of $\text{Ru}(\text{NR}')(\text{MeC}_6\text{H}_4\text{Pr}^i\text{-}p)$ ($\text{R}' = 2,4,6\text{-Bu}^i_3\text{C}_6\text{H}_2$) with $(\text{mes})\text{NCO}$ and $(\text{mes})\text{N}_3$ are reported. Attempts to isolate $\text{Rh}(\eta\text{-C}_5\text{Me}_5)(\text{NR})$ species failed but evidence for $\text{Rh}(\eta\text{-C}_5\text{Me}_5)\text{-}[\text{N}(2,6\text{-Pr}^i_2\text{C}_6\text{H}_3)\text{N}_3(\text{mes})]$ was obtained in a trapping reaction in solution using $(\text{mes})\text{N}_3$. The crystal structures of the compounds $\text{Ir}(\eta\text{-C}_5\text{Me}_5)(\eta^2\text{-Bu}^1\text{NCNBu}^1)(\text{CNBu}^1)$, $[\text{Ir}(\eta\text{-C}_5\text{H}_5)(\mu\text{-NC}_5\text{H}_9)]_2$ **2**, **3**, $[\text{Ir}_2(\eta\text{-C}_5\text{Me}_5)(\mu\text{-NC}_6\text{H}_{11})(\mu\text{-NHC}_6\text{H}_{11})]\text{Cl}$ **3**, $\text{Ir}(\eta\text{-C}_5\text{Me}_5)[\text{N}(\text{xyl})\text{CHN}(2,6\text{-Pr}^i_2\text{C}_6\text{H}_3)\text{CNC}_6\text{H}_3(\text{Me})\text{CH}_2]$ **4b**, $\text{Ir}(\eta\text{-C}_5\text{Me}_5)[\text{N}(2,6\text{-Pr}^i_2\text{C}_6\text{H}_3)\text{C}(\text{O})\text{N}(\text{mes})]$ **5**, $\text{Ir}(\eta\text{-C}_5\text{Me}_5)[\text{N}(2,6\text{-Pr}^i_2\text{C}_6\text{H}_3)\text{N}_3(\text{mes})]$ **6**, $\text{Ru}[\text{N}(2,4,6\text{-Bu}^i_3\text{C}_6\text{H}_2)\text{C}(\text{O})\text{N}(\text{mes})](\text{MeC}_6\text{H}_4\text{Pr}^i\text{-}p)$ **8** and $\text{Ru}[\text{N}(2,4,6\text{-Bu}^i_3\text{C}_6\text{H}_2)\text{N}_3(\text{mes})](\text{MeC}_6\text{H}_4\text{Pr}^i\text{-}p)$ **9** have been determined. A reaction mechanism for the formation of **4b** is given.

It was shown¹ that the interaction of the chromium(III) compound $\text{Cr}(\eta\text{-C}_5\text{Me}_5)(=\text{NC}_6\text{H}_3\text{Pr}^i\text{-}2,6)$ generated *in situ*, with an excess of 2,6-xylyl isocyanide in tetrahydrofuran gave the compound shown in diagram I. Since the mechanism proposed for the formation involved sequential coupling of three isocyanide molecules it seemed likely that similar insertions into the metal imido bonds could occur with the nucleophilic imido complexes of iridium(III),² $\text{Ir}(\eta\text{-C}_5\text{Me}_5)(=\text{NR})$ ($\text{R} = \text{Bu}^1$ **1a** or 2,6- $\text{Pr}^i_2\text{C}_6\text{H}_3$ **1b**). Reactions of these imido complexes and of the ruthenium(II) complex, $\text{Ru}(=\text{NC}_6\text{H}_2\text{Bu}^i\text{-}2,4,6)(\eta\text{-MeC}_6\text{H}_4\text{Pr}^i\text{-}p)$,³ with 2,6-xylyl isocyanide, $(\text{mes})\text{NCO}$ and $(\text{mes})\text{N}_3$ (mes = $\text{C}_6\text{H}_2\text{Me}_3$ -2,4,6) are now described. Attempts to obtain rhodium analogues from $\text{Rh}(\eta\text{-C}_5\text{Me}_5)(\text{NR})$ species made *in situ* were unsuccessful. Physical and analytical data for new compounds are given in Table 1.

Results and Discussion

Iridium complexes

The interaction of compound **1a** with Bu^1NC produces the previously reported carbodiimide compound $\text{Ir}(\eta\text{-C}_5\text{Me}_5)(\eta^2\text{-Bu}^1\text{NCNBu}^1)(\text{CNBu}^1)$, whose structural formulation was based on IR and NMR data.^{2a} In view of the quite different products obtained when 2,6-xylyl isocyanide is used with either **1a** or **1b** as discussed below, the η^2 -carbodiimide structure was confirmed by X-ray diffraction. The structure was solved and successfully refined in the monoclinic space group $P2_1/m$. A diagram of the structure is given in Fig. 1, with selected bond lengths and angles in Table 2. The C_5Me_5 and terminal isocyanide ligands are bisected by the mirror plane, which also contains the metal; it also relates the two Bu^1 groups on the carbodiimide. Atom C(20) of this ligand also lies on the mirror plane but the nitrogen N(2) is equally disordered over two sites, thus modelling the asymmetry of the N–C–N grouping arising out of the η^2 C–N bonding. Detailed discussion of the bonding of this ligand is not possible since it was necessary to constrain the positions of the two half-nitrogens to achieve realistic N–C (Bu^1) distances.

In order to find out if carbodiimides were formed in other cases, we first synthesized the cyclopentylimido complex $[\text{Ir}(\eta\text{-C}_5\text{Me}_5)(\mu\text{-NC}_5\text{H}_9)]_2$ **2** using reaction conditions similar to those described.² The structure was confirmed by X-ray

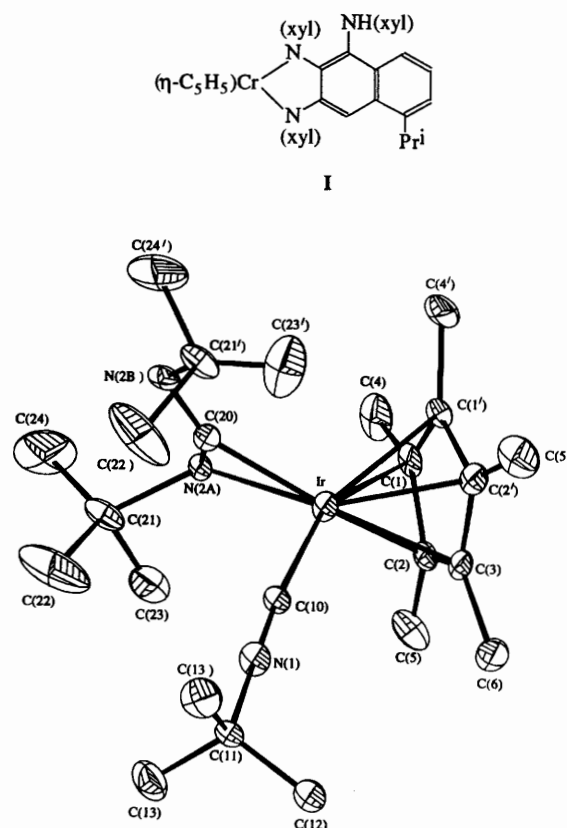


Fig. 1 The structure of $\text{Ir}(\eta\text{-C}_5\text{Me}_5)(\eta^2\text{-Bu}^1\text{NCNBu}^1)(\text{CNBu}^1)$. Primed atoms are related to their unprimed equivalents by the crystallographic mirror plane (see text)

diffraction, see Fig. 2 and Table 3. The core geometry is similar to that found for the phenylimido- and 2,6-dimethylphenylimido-bridged dimers described by Dobbs and Bergman^{2b} in that the Ir_2N_2 group is folded (dihedral angle between the two IrN_2 planes = 76.14°) and the two nitrogens are not planar [angle sums = 339.8° for N(1) and 351.8° for N(2)]. Possible reasons for these features were discussed previously.^{2b} However, the structures show quite significant differences in detail. The $\text{Ir}\cdots\text{Ir}$ distance in **2** is $2.6133(5)$ Å, some $0.14\text{--}0.16$ Å shorter than in the aryl derivatives and the

Table 1 Analytical and physical data for new compounds

Compound	M.p./°C	Analysis (%) [*]		
		C	H	N
2 [Ir(η-C ₅ Me ₅)(μ-NC ₅ H ₉) ₂	209–211	44.0 (43.9)	6.1 (5.9)	3.2 (3.4)
3 [Ir ₂ (η-C ₅ Me ₅) ₂ (μ-NC ₆ H ₁₁)(μ-NHC ₆ H ₁₁)]Cl	187	43.8 (43.4)	6.0 (6.0)	3.0 (3.2)
4a Ir(η-C ₅ Me ₅)[N(xyl)CHN(Bu ^t)CNC ₆ H ₃ (Me)CH ₂]	169–171	58.0 (58.2)	6.2 (6.2)	6.0 (6.4)
4b Ir(η-C ₅ Me ₅)[N(xyl)CHN(2,6-Pr ⁱ ₂ C ₆ H ₃)CNC ₆ H ₃ (Me)CH ₂]	221–225	61.9 (61.7)	6.4 (6.3)	5.4 (5.3)
5 Ir(η-C ₅ Me ₅)[N(2,6-Pr ⁱ ₂ C ₆ H ₃)C(O)N(mes)]	220	57.9 (57.9)	6.7 (6.9)	4.0 (4.2)
6 Ir(η-C ₅ Me ₅)[N(2,6-Pr ⁱ ₂ C ₆ H ₃)N ₃ (mes)]	240 (decomp.)	56.2 (56.1)	6.5 (6.5)	8.2 (8.4)
7 Rh(η-C ₅ Me ₅)[N(2,6-Pr ⁱ ₂ C ₆ H ₃)N ₃ (mes)]	225	64.5 (64.8)	7.5 (7.5)	9.6 (9.8)
8 Ru[N(2,4,6-Bu ^t ₃ C ₆ H ₂)C(O)N(mes)](MeC ₆ H ₄ Pr ⁱ -p)	> 240	69.5 (69.6)	8.2 (8.2)	4.1 (4.3)
9 Ru[N(2,4,6-Bu ^t ₃ C ₆ H ₂)N ₃ (mes)](MeC ₆ H ₄ Pr ⁱ -p)	98–100	67.7 (67.8)	8.2 (8.2)	8.5 (8.5)

* Calculated values in parentheses. Mass spectral data are given in the Experimental section.

Table 2 Selected bond lengths (Å) and angles (°) for Ir(η-C₅Me₅)-(η²-Bu^tNCNBU^t)(CNBU^t) with estimated standard deviations (e.s.d.s) in parentheses

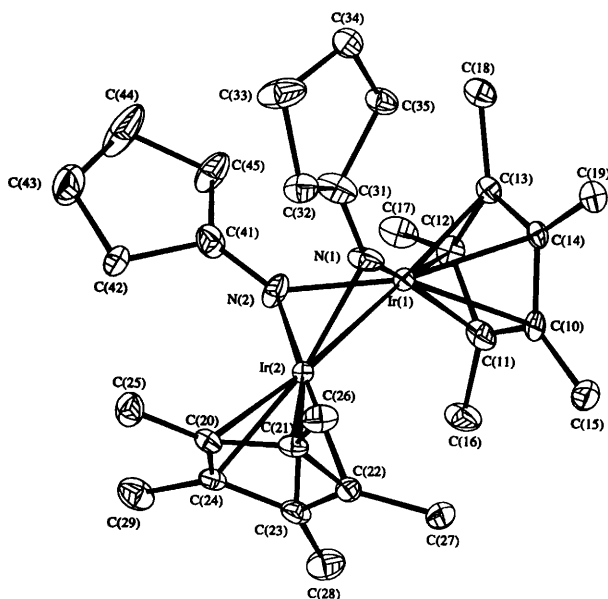
Ir–Cp(1*)	1.89(2)	N(1)–C(10)	1.137(13)
Ir–C(10)	1.900(10)	N(1)–C(11)	1.430(14)
Ir–C(20)	2.017(9)	C(20)–N(2A)	1.199(13)
Ir–N(2A)	2.206(10)		
Cp(1*)–Ir–C(10)	128.9(7)	C(10)–N(1)–C(11)	178.3(10)
Cp(1*)–Ir–N(2A)	123.3(7)	N(1)–C(10)–Ir	174.6(9)
Cp(1*)–Ir–C(20)	139.4(7)	Ir–N(2A)–C(20)	65.0(7)
C(10)–Ir–N(2A)	99.2(3)	Ir–N(2A)–C(21)	137.4(6)
C(10)–Ir–C(20)	91.8(4)	Ir–C(20)–N(2A)	82.4(7)
N(2A)–Ir–C(20)	32.6(3)	Ir–C(20)–N(2B ^t)	137.0(6)

Cp(1*) represents the centroid of the C₅Me₅ ring C(1), C(2), C(3), C(1'), C(2'). Primed atoms are related to unprimed ones by the symmetry transformation $x, -y + \frac{1}{2}, z$.

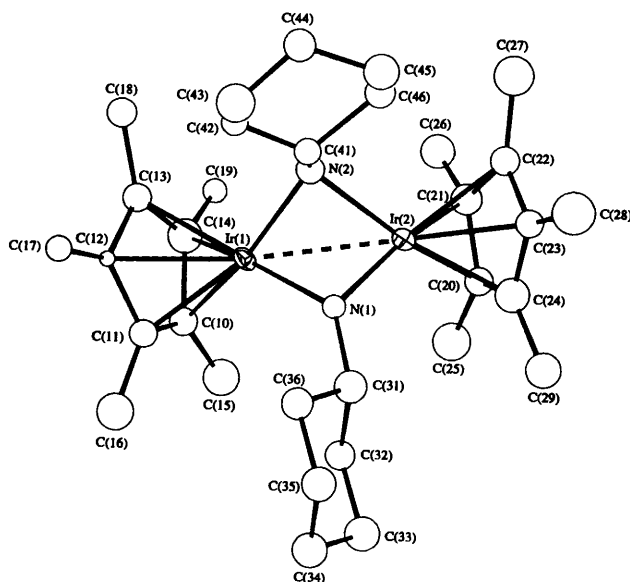
Table 3 Selected bond lengths (Å) and angles (°) for [Ir(η-C₅Me₅)(NC₅H₉)₂]⁺ 2 with e.s.d.s in parentheses

Ir(1)···Ir(2)	2.6133(5)	Ir(2)–N(1)	2.049(7)
Ir(1)–N(1)	2.046(8)	Ir(2)–N(2)	2.029(7)
Ir(1)–N(2)	2.010(8)	Ir(2)–Cp(2*)	1.84(2)
Ir(1)–Cp(1*)	1.83(2)		
N(1)–Ir(1)–N(2)	74.4(3)	N(1)–Ir(2)–Cp(2*)	142.9(8)
N(1)–Ir(1)–Cp(1*)	139.9(8)	N(2)–Ir(2)–Cp(2*)	141.8(8)
N(2)–Ir(1)–Cp(1*)	144.2(8)	Ir(1)–N(1)–Ir(2)	79.3(3)
N(1)–Ir(2)–N(2)	74.0(3)	Ir(1)–N(2)–Ir(2)	80.6(3)

Cp(1*) represents the centroid of the C₅Me₅ ring C(10)–C(14), Cp(2*) that of the ring C(20)–C(24).

**Fig. 2** The structure of [Ir(η-C₅Me₅)(μ-NC₅H₉)₂]⁺ 2

Ir–N distances are 2.010–2.046(8) Å, compared with 1.97–1.99(1) Å in the aryls. More importantly, the orientations of the cyclopentyl groups in 2 are both approximately parallel to the Ir···Ir vector, whereas in both aryl complexes the rings are perpendicular to this direction. This difference is very significant in that steric interactions between the substituents on the imido functions and the C₅Me₅ groups will be quite different, likely to be much greater in 2. The resulting steric pressure on the C₅Me₅ groups, which are symmetrically η⁵ bound in both complexes, may thus have resulted in the greater folding about the N···N vector in 2 leading to a shorter Ir···Ir bond.

**Fig. 3** The structure of the cation [Ir₂(η-C₅Me₅)₂(μ-NC₆H₁₁)(μ-NHC₆H₁₁)]⁺ in 3

Unfortunately compound 2 was unreactive towards cyclohexyl isocyanide and *tert*-butyl isocyanide even with prolonged refluxing in tetrahydrofuran.

In addition, interaction of [Ir(η-C₅H₅)Cl₂]₂ with 3 equivalents of Li(NHC₆H₁₁) in thf as above gave low yields of 3, a dimeric, cationic species with one cyclohexylimido and one cyclohexylamido function. Its identity was established by analytical, spectroscopic (¹H NMR) and crystallographic studies. Although the crystals were of poor quality, the structure determination clearly identifies all main features. A diagram of the cation is shown in Fig. 3, whilst bond lengths and angles are given in Table 4. The dimer cation has the same kind of folded (C₅Me₅)IrN₂Ir(C₅Me₅) feature found for 2, with differences in detail, as might be expected. The differences in the bridging groups are easily identified, with N(1) the imido

nitrogen giving N–Ir distances of 1.85(3) and 1.92(3) Å, and an angle sum of 356.6°. The amido nitrogen, N(2), gives distances to Ir of 2.02(3) and 2.11(3) Å, and has an angle sum of 319.4°. The cyclohexyl group on the amido is oriented in the 'parallel' mode, whilst that on the imido is roughly in the perpendicular orientation. We presume that the net effect is to reduce steric interactions with the C₅Me₅ groups, since the fold at the N···N vector 67.7° is smaller than in **2**, and the Ir···Ir bond longer, at 2.724(2) Å.

As noted above compounds **1a** and **1b** show different behaviour when 2,6-xylyl isocyanide is employed. In tetrahydrofuran essentially quantitative (by NMR) yields of the compounds **4a** and **4b** are obtained; both have the structure shown. The structure of **4b** was determined by X-ray diffraction and is shown in Fig. 4; bond lengths and angles are given in Table 5. For the most part the bond lengths and angles in the tridentate ligand are consistent with the formalized structure shown except that the planar amine nitrogen [N(2)] shows some π conjugation with the imine system involving N(3); thus the N(2)–C(101) and C(101)–N(3) distances are both short; N(2)–C(100), however, is similar to a single bond. The presence of the saturated, methylene carbon [C(121)] in the six-membered chelate ring gives this ring some flexibility, so that it is folded at the N(1)···C(121) vector and the chelate bite angle is smaller, at 74.8(2)°, than the bite angle [77.1(2)°] in the planar five-membered chelate ring. The Ir–N and Ir–C distances associated with this ligand all indicate

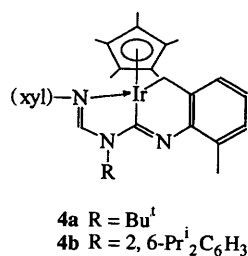


Table 4 Selected bond lengths (Å) and angles (°) for the cation [Ir₂(η-C₅Me₅)₂(μ-NC₆H₁₁)(μ-NHC₆H₁₁)]⁺ in compound **3** with e.s.d.s in parentheses

Ir(1)···Ir(2)	2.724(2)	Ir(2)–N(1)	1.85(3)
Ir(1)–N(1)	1.92(3)	Ir(2)–N(2)	2.11(3)
Ir(1)–N(2)	2.02(3)	Ir(2)–Cp(2*)	1.86(10)
Ir(1)–Cp(1*)	1.61(11)		
N(1)–Ir(1)–N(2)	74.0(11)	N(1)–Ir(2)–Cp(2*)	143(3)
N(1)–Ir(1)–Cp(1*)	148(4)	N(2)–Ir(2)–Cp(2*)	144(3)
N(2)–Ir(1)–Cp(1*)	137(4)	Ir(1)–N(1)–Ir(2)	92.6(11)
N(1)–Ir(2)–N(2)	73.2(11)	Ir(1)–N(2)–Ir(2)	82.4(10)

Cp(1*) and Cp(2*) as in Table 3.

Table 5 Selected bond lengths (Å) and angles (°) for Ir(η-C₅Me₅)[N(xy)CHN(2,6-Prⁱ₂C₆H₃)CNC₆H₃(Me)CH₂]**4b** with e.s.d.s in parentheses

Ir–C(121)	2.114(6)	N(2)–C(100)	1.433(7)
Ir–C(100)	2.019(6)	C(100)–N(1)	1.277(7)
Ir–N(3)	2.102(5)	N(1)–C(11)	1.435(7)
Ir–Cp(1*)	1.873(13)	C(11)–C(12)	1.421(8)
N(3)–C(101)	1.303(7)	C(12)–C(121)	1.502(9)
C(101)–N(2)	1.348(8)		
C(121)–Ir–C(100)	74.8(2)	N(3)–C(101)–N(2)	119.4(6)
C(121)–Ir–N(3)	95.0(2)	C(101)–N(2)–C(100)	113.3(5)
C(121)–Ir–Cp(1*)	126.3(6)	N(2)–C(100)–N(1)	113.6(5)
C(100)–Ir–N(3)	77.0(2)	C(100)–N(1)–C(11)	116.4(5)
C(100)–Ir–Cp(1*)	136.0(5)	N(1)–C(11)–C(12)	119.0(5)
N(3)–Ir–Cp(1*)	129.1(5)	C(11)–C(12)–C(121)	119.5(5)
Ir–N(3)–C(101)	112.7(4)	C(12)–C(121)–Ir	109.5(4)

Cp(1*) represents the centroid of the C₅Me₅ ring C(1)–C(5).

normal single bonds. The C₅Me₅ ligand shows slight tilting, with Ir–C distances of 2.186(7)–2.269(6) Å.

The NMR data are consistent with the structure in both cases; assignments of the complicated ¹H spectra were carried out using two-dimensional correlation spectroscopy (COSY). Thus for both compounds **4a** and **4b** the methyl groups on the xylylimino group are diastereotopic giving rise to two separate resonances. The same applies to the methylene protons giving rise to an AB doublet of doublets. In addition, for **4b**, the isopropyl methyls are inequivalent producing four doublets. The resonances of the remaining protons, e.g. of the C₅Me₅ groups, methyls on cyclometallated xylyl, aromatics and *tert*-butyl (for **4a**), are in normal positions.

A mechanism for the formation of these compounds is shown in Scheme 1. The first step, a [2 + 2] cycloaddition, is the same as that proposed for the reaction of Cr(η-C₅Me₅) (=NR) with isocyanide¹ and leads to the carbene intermediate A. Highly stabilized carbenes of the type shown in diagram II are well known in organic chemistry^{4a} and as >C:→M donors in

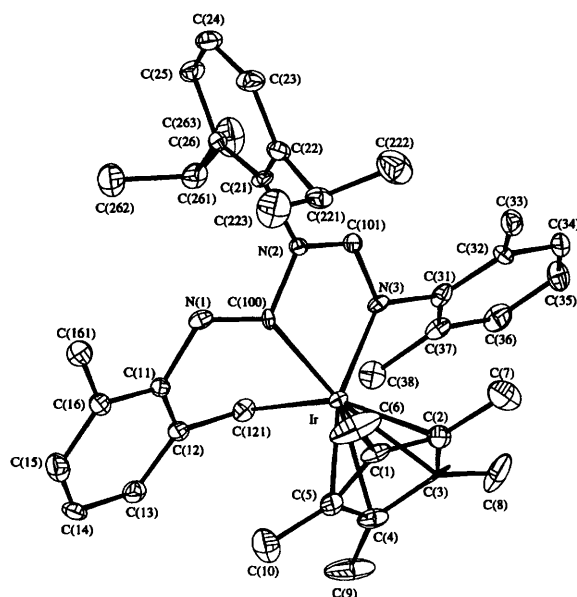
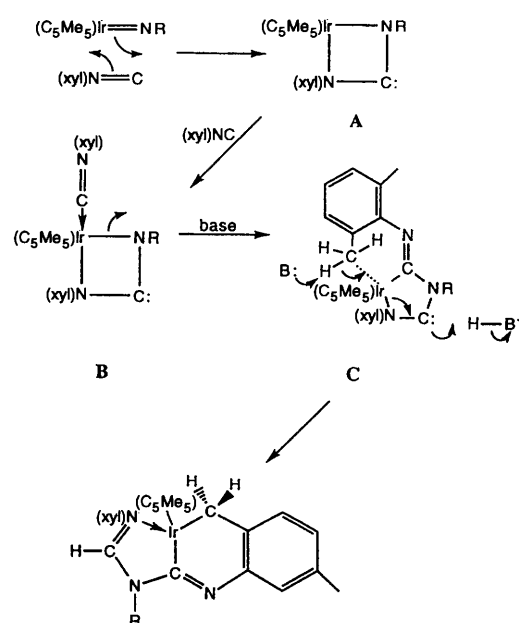


Fig. 4 The structure of Ir(η-C₅Me₅)[N(xy)CHN(2,6-Prⁱ₂C₆H₃)CNC₆H₃(Me)CH₂]**4b**



Scheme 1 R = 2,6-Prⁱ₂C₆H₃

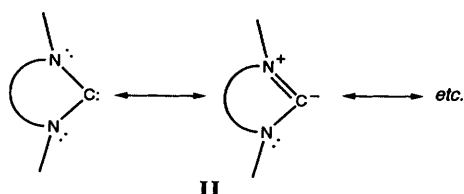


Table 6 Selected bond lengths (Å) and angles (°) for Ir(η -C₅Me₅)[N(2,6-Prⁱ₂C₆H₃)C(O)N(mes)] **5** with e.s.d.s in parentheses

Ir–N(1)	1.92(2)	N(1)–C(100)	1.56(2)
Ir–N(2)	2.03(2)	N(2)–C(21)	1.39(2)
Ir–Cp(1*)	1.83(3)	N(2)–C(100)	1.41(3)
N(1)–C(11)	1.27(3)	C(100)–O	1.18(2)
N(1)–Ir–N(2)	68.0(7)	C(21)–N(2)–C(100)	123(2)
N(1)–Ir–Cp(1*)	151.7(1)	Ir–N(2)–C(100)	98.0(13)
N(2)–Ir–Cp(1*)	140.9(11)	Ir–N(2)–C(21)	138.1(14)
C(11)–N(1)–C(100)	116(2)	N(1)–C(100)–N(2)	96(2)
Ir–N(1)–C(100)	97.8(13)	N(1)–C(100)–O	129(2)
Ir–N(1)–C(11)	147(2)	N(2)–C(100)–O	135(2)

Cp(1*) as in Table 5.

complexes of low-valent metals such as Ni⁰, Pt⁰,^{4b} Sm^{II}, Eu^{III}, Yb^{II}^{4c} and Pd^{II}.^{4d} This step is then followed by isocyanide coordination and insertion into the Ir–N< bond to give **B**. Required now is a sequence of transfers as in **C** where a base, presumably the isocyanide, deprotonates the *o*-CH₃ group on the xylyl ring leading to formation of the C–CH₂–Ir moiety. The hydrogen on B⁺–H is then transferred to the carbene C atom with concomitant formation of a (xyl)N=C bond and a donor $\ddot{N}:$ →Ir bond. There is no change in the oxidation state of iridium in these sequences.

The interaction of the imido compound **1b** with mesityl isocyanate at 110 °C in octane gives moderate yields of the blue, air-stable asymmetric *N,N'*-diarylureato⁵ complex Ir(η -C₅Me₅)[N(2,6-Prⁱ₂C₆H₃)C(O)N(mes)] **5**. Under similar conditions **1a** with (mes)NCO gives only intractable mixtures; the compound Os^{II}(NBu^t)(MeC₆H₄Prⁱ-*p*) on reaction with Bu^tNCO does, however, give a ureato complex.⁶

The structure of compound **5** was determined by X-ray crystallography and is shown in Fig. 5; bond lengths and angles are in Table 6. The crystal quality for this determination was poor, and the resulting accuracy of structural parameters low. Nevertheless the main features are quite clear. The ureate ligand bonds in an almost symmetrical fashion. The Ir–N and Ir–C (C₅Me₅) distances are very similar to those in the isoelectronic complex Ir(η -C₅Me₅)[NBu^tC(O)O] described by Bergman and co-workers.^{2a} The C₅Me₅ bonding is symmetrical pentahapto in both complexes; in the other ligands the substituents on the N atoms give large Ir–N–C angles (> 140°) in both cases. However, other parameters indicate that this is a feature of strain (*i.e.* 'bent-bonding overlap') in the Ir–N bonding, arising from the small ligand bite, rather than any steric strain involving the substituent groups and the C₅Me₅.

The interaction of compound **1b** with mesityl azide in tetrahydrofuran (thf) at room temperature produces the *N,N'*-diaryltetrazene⁷ complex **6** by the usual 1,3-dipolar cycloaddition in Scheme 2. The structure determined by X-ray diffraction is shown in Fig. 6; bond lengths and angles are in Table 7. The five-membered IrN₄ ring has almost equal Ir–N bond lengths and although the double bond seems to be localized at N(2)–N(3) [1.277(7) Å], N(1) and N(4) are planar while the N(1)–N(2) and N(3)–N(4) distances are slightly shorter than expected for normal single bonds; this indicates some electron delocalization over the four N atoms. The C₅Me₅ ligand bonds symmetrically, with Ir–C distances differing only by 0.02 Å. The ¹H NMR spectrum has bands for mesityl and 2,6-disopropylphe-

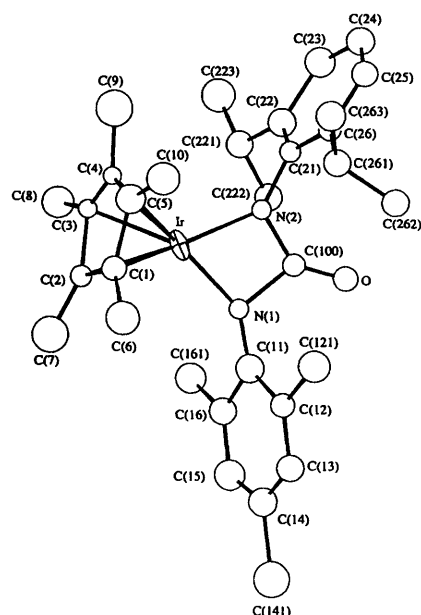


Fig. 5 The structure of Ir(η -C₅Me₅)[N(2,6-Prⁱ₂C₆H₃)C(O)N(mes)] **5**



Scheme 2 R = 2,6-Prⁱ₂C₆H₃

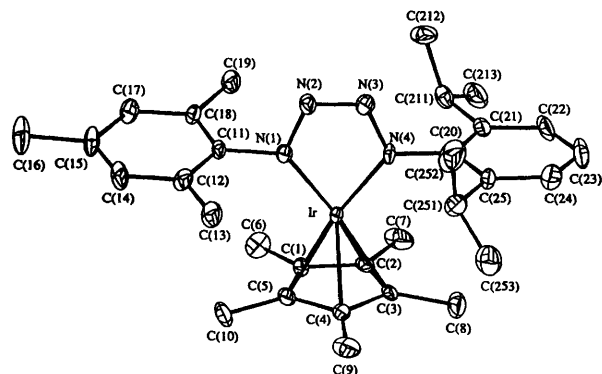


Fig. 6 The structure of Ir(η -C₅Me₅)[N(2,6-Prⁱ₂C₆H₃)N₃(mes)] **6**

Table 7 Selected bond lengths (Å) and angles (°) for Ir(η -C₅Me₅)[N(2,6-Prⁱ₂C₆H₃)N₃(mes)] **6** with e.s.d.s in parentheses

Ir–N(1)	1.925(5)	N(1)–C(11)	1.451(8)
Ir–N(4)	1.940(5)	N(2)–N(3)	1.277(7)
Ir–Cp(1*)	1.821(14)	N(3)–N(4)	1.367(6)
N(1)–N(2)	1.371(6)	N(4)–C(20)	1.441(8)
N(1)–Ir–N(4)	74.1(2)	N(1)–N(2)–N(3)	112.2(5)
N(1)–Ir–Cp(1*)	143.5(6)	N(2)–N(3)–N(4)	113.0(5)
N(4)–Ir–Cp(1*)	142.5(6)	N(3)–N(4)–C(20)	113.0(5)
N(2)–N(1)–C(11)	111.2(5)	N(3)–N(4)–Ir	119.9(4)
Ir–N(1)–C(11)	127.9(4)	C(20)–N(4)–Ir	127.0(4)
Ir–N(1)–N(2)	120.8(4)		

Cp(1*) as in Table 5.

nyl groups in a 1 : 1 ratio and the isopropyl methyl groups are diastereotopic, as found for **5**. The electron impact (EI) mass spectrum shows the molecular ion. There is no sign of cleavage of the tetrazene moiety thermally or on photolysis even in the presence of donors such as PMe₃. Tetrazene osmium complexes

have been obtained by reaction of $\text{Os}(\text{NBu}^i)(\text{MeC}_6\text{H}_4\text{Pr}^i\text{-}p)$ with azides.⁶

Rhodium complexes

Attempts to isolate rhodium analogues of **1a** and **1b** have failed. At temperatures above *ca.* 5 °C the red-brown solutions from the reactions of $[\text{Rh}(\eta\text{-C}_5\text{Me}_5)\text{Cl}_2]_2$ ⁸ and various lithium amido compounds, $\text{Li}(\text{NHR})$ (R = alkyl and aryl), that may possibly contain $\text{Rh}(\eta\text{-C}_5\text{Me}_5)(\text{NR})$ species, decomposed to give purple solutions which on evaporation leave solids giving purple solutions in hexane. Crystals could not be obtained from a range of solvents. The NMR spectra were uninterpretable and addition of compounds such as tertiary phosphines, pyridine, *etc.*, gave no identifiable adducts. Attempts to isolate $\text{Rh}(\eta\text{-C}_5\text{Me}_5)(\text{NR})$ species at low temperatures in polar or non-polar solvents also failed.

The only indication that $\text{Rh}(\eta\text{-C}_5\text{Me}_5)(\text{C}_6\text{H}_3\text{Pr}^i\text{-}2,6)$ could exist, for a short time at any rate at 0 °C, was the interaction with $(\text{mes})\text{N}_3$ immediately after generation which produced the rhodium tetrazene complex **7**, which is analogous to that of iridium and has similar spectroscopic properties. The yellow-brown crystalline product was air-stable; the mass spectrum showed the molecular ion. The cobalt analogue $\text{Co}(\eta\text{-C}_5\text{Me}_5)[(\text{mes})\text{N}_4(2,6\text{-Pr}^i\text{-C}_6\text{H}_3)]$ has been made similarly by H. Petersen in these laboratories.

We have also tried to obtain imido species starting with other materials: $[\text{Rh}(\eta\text{-C}_5\text{H}_5)\text{Cl}_2]_n$,^{9a} $\{\text{Rh}[\text{HB}(\text{dmpz})_3]\text{Cl}_2\}_2$ ^{9b}

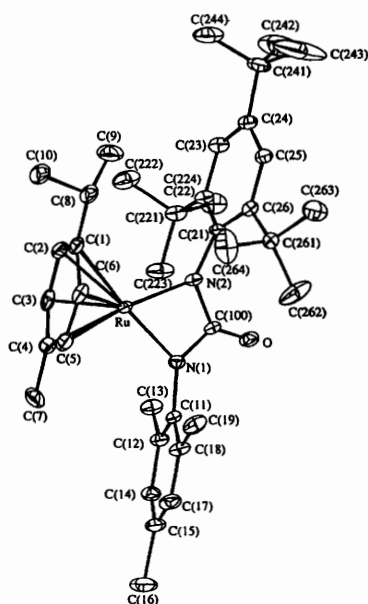


Fig. 7 The structure of $\text{Ru}[\text{N}(2,4,6\text{-Bu}_3\text{C}_6\text{H}_2)\text{C}(\text{O})\text{N}(\text{mes})]\text{-}(\text{MeC}_6\text{H}_4\text{Pr}^i\text{-}p)$ **8**

Table 8 Selected bond lengths (Å) and angles (°) for $\text{Ru}[\text{N}(2,4,6\text{-Bu}_3\text{C}_6\text{H}_2)\text{C}(\text{O})\text{N}(\text{mes})]\text{-}(\text{MeC}_6\text{H}_4\text{Pr}^i\text{-}p)$ **8** with e.s.d.s in parentheses

Ru–N(1)	1.988(4)	N(1)–C(100)	1.408(6)
Ru–N(2)	2.023(4)	N(2)–C(21)	1.434(6)
Ru–Cym(1*)	1.681(10)	N(2)–C(100)	1.390(6)
N(1)–C(11)	1.411(6)	C(100)–O	1.218(5)
N(1)–Ru–N(2)	66.1(2)	C(21)–N(2)–C(100)	127.5(4)
N(1)–Ru–Cym(1*)	143.8(4)	Ru–N(2)–C(100)	94.2(3)
N(2)–Ru–Cym(1*)	149.8(4)	Ru–N(2)–C(21)	138.0(3)
C(11)–N(1)–C(100)	128.1(4)	N(1)–C(100)–N(2)	102.8(4)
Ru–N(1)–C(100)	95.2(3)	N(1)–C(100)–O	127.3(4)
Ru–N(1)–C(11)	133.5(3)	N(2)–C(100)–O	129.8(4)

Cym(1*) represents the centroid of the cymene ring C(1)–C(6).

(*dmpz* = 3,5-dimethylpyrazolyl), $\text{Rh}(\eta\text{-C}_5\text{Me}_5)(\text{Me})\text{Br}(\text{P-Me})_3$ ^{9c} and $\text{Rh}(\eta\text{-C}_5\text{Me}_5)(\text{PMe}_3)(\text{O}_3\text{SCF}_3)_2$ ^{9d} under a variety of conditions with the lithium salts from NH_2Bu^i and several aromatic amines, but in all cases intractable materials were obtained.

The reason for the difference in stability or reactivity of the rhodium and iridium compounds is not clear; possibly reduction to unstable or polymeric species is occurring with the rhodium compounds.

Ruthenium complexes

The interaction of $\text{Ru}(\text{NR})(\text{MeC}_6\text{H}_4\text{Pr}^i\text{-}p)$, R = 2,4,6-Buⁱ₃C₆H₂,³ with $(\text{mes})\text{NCO}$ at room temperature shows that this complex is more reactive than the iridium(III) species. The asymmetric ureato complex **8** is obtained as thermally and air-stable blue crystals. The crystal structure is shown in Fig. 7; bond lengths and angles are in Table 8. The structure is as expected, but with small deviations from idealized geometry arising out of some degree of steric strain involving the Prⁱ group on the cymene and Buⁱ groups on the ureate ligand. Thus the cymene ring is tilted slightly, with Ru–C distances varying from 2.139(5) [C(3)] to 2.265(5) Å [C(1)], and Ru–N(2) is some 0.035 Å longer than the Ru–N(1) bond length. The Ru–N(2)–C(21) angle to the R substituent is also *ca.* 5° greater than the equivalent angle Ru–N(1)–C(11), but both are some 10–15° smaller than in the iridium complex **5**. The N–C distances in the ureate ligand are equal.

The interaction of $\text{Ru}(\text{NR})(\text{MeC}_6\text{H}_4\text{Pr}^i\text{-}p)$, R = 2,4,6-Buⁱ₃C₆H₂, with $(\text{mes})\text{N}_3$ gave a yellow-brown tetrazene complex **9**, characterized by analytical and ¹H NMR data. The latter show distinct resonances for mesityl and R groups while the aromatic protons of the η⁶-arene ring appear as a doublet of doublets (AB) indicating that the asymmetric structure is not present in solution, probably because of η⁶-arene ring rotations. The solid-state structure is shown in Fig. 8 and bond lengths and angles are given in Table 9.

The structure and geometry are as expected, in view of the

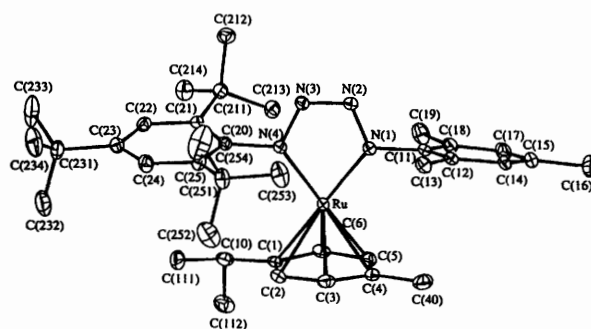


Fig. 8 The structure of $\text{Ru}[\text{N}(2,4,6\text{-Bu}_3\text{C}_6\text{H}_2)\text{N}_3(\text{mes})]\text{-}(\text{MeC}_6\text{H}_4\text{Pr}^i\text{-}p)$ **9**

Table 9 Selected bond lengths (Å) and angles (°) for $\text{Ru}[\text{N}(2,4,6\text{-Bu}_3\text{C}_6\text{H}_2)\text{N}_3(\text{mes})]\text{-}(\text{MeC}_6\text{H}_4\text{Pr}^i\text{-}p)$ **9** with e.s.d.s in parentheses

Ru–N(1)	1.946(3)	N(1)–C(11)	1.439(4)
Ru–N(4)	1.967(3)	N(2)–N(3)	1.288(4)
Ru–Cym(1*)	1.709(8)	N(3)–N(4)	1.358(3)
N(1)–N(2)	1.365(4)	N(4)–C(20)	1.444(4)
N(1)–Ru–N(4)	74.08(11)	N(1)–N(2)–N(3)	112.6(2)
N(1)–Ru–Cym(1*)	140.5(3)	N(2)–N(3)–N(4)	113.7(2)
N(4)–Ru–Cym(1*)	145.4(3)	N(3)–N(4)–C(20)	111.4(2)
N(2)–N(1)–C(11)	112.3(2)	N(3)–N(4)–Ru	119.2(2)
Ru–N(1)–C(11)	127.0(2)	C(20)–N(4)–Ru	129.3(2)
Ru–N(1)–N(2)	120.4(2)		

Cym(1*) as in Table 8.

earlier work on complexes **6** and **7**. The cymene ring is again slightly tilted, with Ru–C distances ranging from 2.170(4) to 2.270(3) Å, the longest to C(1), which is also bound to a Prⁱ substituent. It is interesting that the orientation of the cymene ring, which appears to be fluxional in solution, places the Prⁱ group on the same side as the bulky R substituent, as in complex **6**. The structure of the ruthenium–tetrazene ring is analogous to that found in **6**, with the double bond localized at N(2)–N(3).

The interaction of Ru(NR)(MeC₆H₄Prⁱ-*p*) with isocyanides is very fast even in non-polar solvents like light petroleum and at low temperatures (–78 °C) as judged by changes in the solution from green to brown. Since crystalline products could not be obtained, the reaction with Bu¹NC in [²H₈]toluene was followed by ¹H NMR spectra. Initially a species is formed instantaneously at –60 °C that has one Bu¹NC per ruthenium. Shifts are observed for protons assignable to Bu¹, arylimido and η⁶-arene groups. This species begins to disappear at 0 °C being replaced by that of the final product (or products). The presence of more than one Bu¹NC resonance precludes any reliable conclusions on the nature of the product(s) and no crystals could be isolated.

Experimental

Analyses were by the Imperial College microanalytical laboratory. All operations were carried out under purified Ar or N₂, under vacuum or in a Vacuum Atmospheres glove-box. General techniques have been described.¹⁰

The NMR data were obtained on a JEOL EX-270 or a Bruker Avance DRX 300 spectrometer operating at 270 and 300 MHz (¹H) respectively and referenced to the residual ¹H impurity in the solvent (δ 7.15, C₆D₆; 7.26, CDCl₃). Mass spectra were recorded using VG-7070E (EI) and V. G. Autospec spectrometers. Commercial chemicals were from Aldrich and Fluka. The light petroleum used had b.p. 40–60 °C.

Mesityl isocyanate¹¹ and mesityl azide¹² were made as referenced.

Bis[μ-(cyclopentylimido)(η-pentamethylcyclopentadienyl)iridium(III)] **2**

To a solution of [Ir(η-C₅Me₅)Cl₂]₂ in thf (0.3 g, 0.37 mmol in 30 cm³) at –78 °C was added a solution of Li(NHC₅H₉) (0.14 g, 1.5 mmol) in thf (*ca.* 10 cm³). The reaction suspension was allowed to warm to room temperature and stirred for 2 h giving an orange solution. Evaporation of volatiles under reduced pressure, extraction of the residue in hot light petroleum (3 × 30 cm³), filtration and concentration of extracts and cooling (–20 °C) gave orange prisms. Yield: 0.1 g, *ca.* 35%. NMR (C₆D₆): ¹H, δ 2.1 (s, 30 H, C₅Me₅), 1.2, 1.5, 1.8 and 2.5 (groups of broad multiplets, 18 H, C₅H₉N).

μ-(Cyclohexylamido)-μ-(cyclohexylimido)-bis(η-pentamethylcyclopentadienyl)diiridium(III) chloride **3**

To a solution of [Ir(η-C₅Me₅)Cl₂]₂ (0.3 g, 0.37 mmol) in thf (*ca.* 30 cm³) at –78 °C was added a solution of Li(NHC₆H₁₁) (0.12 g, 1.1 mmol) in thf (*ca.* 10 cm³). The suspension was allowed to warm to room temperature and stirred for 1 h giving a yellow-orange solution. Evaporation of volatiles under reduced pressure, extraction of the residue in hot light petroleum (3 × 30 cm³), filtration, concentration of extracts and cooling (–20 °C) gave orange crystals. Yield: 0.08 g, 25%. NMR (C₆D₆): ¹H, δ 10.6 [s br, 1 H, NH(C₆H₁₁)], 2.0 (s, 30 H, C₅Me₅) and 1.8–1.2 (m, 22 H, C₆H₁₁).

Interaction of Ir(η-C₅Me₅)(NBu¹) with 2,6-xylyl isocyanide to give compound **4a**

To a solution of Ir(η-C₅Me₅)(NBu¹) (0.25 g, 0.63 mmol) in thf (20 cm³) was added a solution of xylyl isocyanide (0.25 g, 1.9

mmol) in thf (15 cm³). The yellow-orange reaction mixture was refluxed for 2 h and the volatiles removed under reduced pressure. The yellow-orange residue was recrystallized from hot light petroleum. Yield: 0.3 g, 72%. Mass spectrum (EI): *m/z* 660 (*M*⁺ + 1) and 604 (*M*⁺ + 1 – isobutylene). NMR (C₆D₆): ¹H, δ 7.5–7.0 (m, 6 H, aromatic), 3.0 and 2.5 (d, 2 H, IrCH₂C₆H₃Me), 2.75, 2.51 and 2.1 (s, 3 H each, xylyl methyl), 1.47 (s, 9 H, NCM₃) and 1.33 (s, 15 H, C₅Me₅).

Interaction of Ir(η-C₅Me₅)(NC₆H₃Prⁱ-2,6) with 2,6-xylyl isocyanide to give compound **4b**

Compound **4b** was prepared as for **4a** from Ir(η-C₅Me₅)(NC₆H₃Prⁱ-2,6) (0.3 g, 0.6 mmol) and 2,6-xylyl isocyanide (0.24 g, 1.8 mmol). After evaporating the thf solution the yellow residue was recrystallized from diethyl ether. Yield: 0.37 g, 80%. Mass spectrum (EI): *m/z* 765 (*M*⁺ + 1) and 635 [*M*⁺ + 1 – C₆H₃(Me)CH₂]. NMR (C₆D₆): ¹H, δ 7.6–6.90 (m, 9 H, aromatic), 3.60 and 3.10 (spt, 1 H each, Me₂CH), 3.40 and 2.55 (doublet of doublets, 2 H, IrCH₂C₆H₃Me), 2.45, 2.40 and 2.0 (s, 3 H each, xylyl methyl), 1.65, 1.40, 1.15 and 1.00 (d, 3 H each, Me₂CH) and 1.38 (s, 15 H, C₅Me₅).

[N-(2,6-Diisopropylphenyl)-N'-(2,4,6-trimethylphenyl)-ureato](η-pentamethylcyclopentadienyl)iridium(III) **5**

A solution of compound **1b** (0.25 g, 0.5 mmol) and (mes)NCO 0.1 g, (*ca.* 0.6 mmol) in octane was heated at 110 °C for 48 h. After removal of octane under reduced pressure the blue residue was recrystallized from light petroleum to yield 0.21 g (*ca.* 65%) of green-blue **5**. NMR (C₆D₆): ¹H, δ 7.3 (m, 3 H, aromatic), 6.9 (s, 2 H, aromatic), 3.8 (spt, 2 H, CHMe₂), 2.6 (s, 6 H, *o*-Me), 2.3 (s, 3 H, *p*-Me), 1.45 (doublet of doublets, 12 H, CHMe₂) and 1.05 (s, 15 H, C₅Me₅). IR (Nujol): 1650 cm^{–1} [ν(C=O)].

[1-(2,6-Diisopropylphenyl)-4-(2,4,6-trimethylphenyl)-tetrazene-1,4-diyl](η-pentamethylcyclopentadienyl)iridium(III) **6**

To a solution of compound **1b** (0.25 g, 0.5 mmol) in thf (20 cm³) was added *via* cannula a thf solution of (mes)N₃ (0.1 g, 0.6 mmol in 5 cm³). The yellow reaction solution was stirred at room temperature for 12 h. Removal of volatiles under reduced pressure and crystallization of the residue from light petroleum gave yellow needles. Yield: 0.28 g, 85%. Mass spectrum (EI): *m/z* 636 (*M*⁺ – 28) and 622 (*M*⁺ – 42). NMR (C₆D₆): ¹H, δ 7.3 (m, 3 H, aromatic), 6.9 (s, 2 H, aromatic), 3.3 (spt, 2 H, CHMe₂), 2.4 (s, 3 H, *p*-Me), 2.2 (s, 6 H, *o*-Me), 1.4 (doublet of doublets, 12 H, CHMe₂) and 1.30 (s, 15 H, C₅Me₅).

[1-(2,6-Diisopropylphenyl)-4-(2,4,6-trimethylphenyl)tetrazene-1,4-diyl](η-pentamethylcyclopentadienyl)rhodium(III) **7**

To a mixture of [Rh(η-C₅Me₅)Cl₂]₂ in thf (0.25 g, 0.4 mmol in 30 cm³) at –78 °C was added a solution of Li[NH(C₆H₃Prⁱ-2,6)] (0.3 g, 1.62 mmol) in thf (10 cm³). The suspension was allowed to warm to 0 °C when all solids dissolved. Stirring at this temperature was continued for *ca.* 0.5 h and the red-brown reaction mixture was cooled again to –78 °C and a solution of (mes)N₃ (0.07 g) in thf (5 cm³) was added dropwise *via* cannula. After completion of the addition the reaction mixture was allowed to warm and stirred at room temperature for 0.5 h. Removal of volatiles under reduced pressure, followed by extraction of volatiles with light petroleum (3 × 30 cm³), filtration, concentration to *ca.* 25 cm³ and cooling gave yellow-brown crystals. Yield: 0.1 g, 45%. Mass spectrum (EI): *m/z* 574 (*M*⁺) and 546 (*M*⁺ – N₂). NMR (C₆D₆): ¹H, δ 7.4 (m, 3 H, aromatic), 6.9 (s, 2 H, aromatic), 3.2 (spt, 2 H, CHMe₂), 2.4 (s, 3 H, *p*-Me), 2.2 (s, 6 H, *o*-Me), 1.4 (doublet of doublets, 12 H, CHMe₂) and 1.30 (s, 15 H, C₅Me₅).

Table 10 Crystal data and structure refinement details for the carbodiimide and compounds **2**, **3**, **4b**, **5**, **6**, **8** and **9**

Formula	2	3	4b	5	6	8	9
M_r	564.84	885.61	765.03	663.90	663.89	691.98	691.98
Crystal system	Monoclinic	Monoclinic	Monoclinic	Triclinic	Trigonal	Monoclinic	Monoclinic
Space group	$P2_1/m$	$P2_1/n$	$P2_1/n$	$P\bar{1}$	$R\bar{3}$	$P2_1/c$	$P2_1/c$
$a/\text{Å}$	9.708(1)	12.036(6)	9.811(6)	8.58(1)	42.90(2)	9.487(6)	9.203(5)
$b/\text{Å}$	15.001(2)	21.539(10)	17.068(8)	11.22(3)	42.90(2)	14.579(9)	14.373(8)
$c/\text{Å}$	9.965(1)	12.388(1)	21.174(10)	15.91(3)	8.400(1)	28.283(6)	28.699(7)
$\alpha/^\circ$				83.51(6)			
$\beta/^\circ$	118.67(1)	93.70(3)	94.99(8)	87.89(7)			
$\gamma/^\circ$				79.4(2)			
$U/\text{Å}^3$	1273(2)	3205(2)	3532(3)	1496(5)	120	3896(4)	3783(3)
Z	2	4	4	2	18	4	4
$D_c/\text{Mg m}^{-3}$	1.473	1.835	1.439	1.474	1.482	1.180	1.215
$F(000)$	568	1720	1552	668	6012	1476	1476
Crystal colour	Beige	Orange	Yellow	Turquoise	Yellow	Turquoise	Orange
Crystal size/mm	$0.24 \times 0.09 \times 0.05$	$0.15 \times 0.12 \times 0.06$	$0.12 \times 0.12 \times 0.09$	$0.12 \times 0.09 \times 0.02$	$0.48 \times 0.05 \times 0.03$	$0.36 \times 0.30 \times 0.18$	$0.42 \times 0.39 \times 0.18$
$\mu(\text{Mo-K}\alpha)/\text{mm}^{-1}$	5.075	8.114	3.680	4.334	4.357	0.402	0.445
Reflections collected	5329	9459	12 543	5920	16 563	14 434	11 565
Independent reflections (R_{int})	1993, 0.0852	4580, 0.1851	5301, 0.0563	4029, 0.1311	4605, 0.0606	5566, 0.0832	5439, 0.0685
Maximum, minimum correction factors	1.289, 0.840	1.241, 0.715	1.042, 0.870	1.359, 0.769	1.139, 0.876	1.151, 0.735	1.117, 0.841
Data, restraints, parameters	1991, 0, 156	4577, 0, 174	5298, 0, 453	4025, 0, 162	4602, 0, 365	5562, 0, 437	5433, 0, 431
Goodness of fit, χ^2	0.985	0.994	0.732	0.700	0.815	0.986	1.026
Observed data [$I > 2\sigma(I)$]	1597	2483	3502	1500	3322	4111	4894
$R1, wR2$ [$I > 2\sigma(I)$]	0.0440, 0.0979	0.1162, 0.2590	0.0312, 0.0559	0.0762, 0.1519	0.0311, 0.0600	0.0541, 0.1290	0.0495, 0.1231
(all data)	0.0550, 0.1025	0.1827, 0.2899	0.0613, 0.0613	0.1612, 0.1930	0.0552, 0.0648	0.0743, 0.1377	0.0544, 0.1284
Largest difference peak and hole/ $e \text{ Å}^{-3}$	1.717, -1.118	8.687, -3.509	1.868, -0.607	1.784, -1.352	3.797, -0.612	1.349, -0.543	2.150, -0.549

$S = [\sum w(F_o^2 - F_c^2)^2 / (n - p)]^{1/2}$, $R1 = \sum |F_o - F_c| / \sum F_o$, $wR2 = [\sum w(F_o^2 - F_c^2)^2 / \sum w(F_o^2)]^{1/2}$, $w = 1 / [\sigma^2(F_o^2) + (xP)^2 + gP]$ and $P = [\max(F_o^2) + 2(F_c^2)]/3$, where n = number of reflections and p = total number of parameters, $x = 0.0524, 0.0615, 0.1220, 0, 0.0188, 0.0058, 0.0670$ and 0.1018 for the carbodiimide and compounds **2**, **3**, **4b**, **5**, **6**, **8** and **9** respectively and $g = 0$ in each case.

η^6 -(*p*-Cymene)[*N*-(2,4,6-tri-*tert*-butylphenyl)-*N'*-(2,4,6-trimethylphenyl)ureato]ruthenium(II) **8**

To a solution of (*p*-cymene)(2,4,6-tributylphenylimido)ruthenium³ in thf (0.3 g, 0.61 mmol in 20 cm³) at room temperature was added a solution of (mes)NCO (0.1 g, 0.65 mmol) in thf (10 cm³). The green solution became green-brown and after stirring at room temperature for ca. 2 h, evaporation of volatiles under reduced pressure, extraction of the residue with light petroleum (2 × 20 cm³), filtration, concentration of filtrates (to ca. 5 cm³) and cooling (−20 °C) gave blue crystals. Yield: 0.14 g, 40%. Mass spectrum (FAB): *m/z* 665 (*M*⁺) and 503 [*M*⁺ − (mes)NHCO]. NMR (C₆D₆): ¹H, δ 7.6 (s, 2 H, aromatic), 6.9 (s, 2 H, aromatic), 4.6–4.4 (doublet of doublets, 4 H, η^6 -Pr¹C₆H₄Me), 2.6 (s, 6 H, *o*-Me₂C₆H₂Me), 2.3 (s, 3 H, *p*-MeC₆H₂Me₂), 1.8 (s, 18 H, *o*-Bu¹₂C₆H₂Bu¹), 1.4 (s, 9 H, *p*-Bu¹C₆H₂Bu¹₂) and 0.7 (d, 6 H, η^6 -Pr¹C₆H₄Me). IR (Nujol): 1655 cm^{−1} [ν (C=O)].

η^6 -(*p*-Cymene)[1-(2,4,6-tri-*tert*-butylphenyl)-4-(2,4,6-trimethylphenyl)tetrazene-1,4-diyl]ruthenium(II) **9**

To a solution of (*p*-cymene)(2,4,6-tri-*tert*-butylphenylimido)ruthenium in light petroleum (0.3 g, 0.61 mmol in 40 cm³) at −78 °C was added a solution of (mes)N₃ in the same solvent (0.1 g, 0.65 mmol in 20 cm³). The green solution, which became brown between −78 and 0 °C, was stirred at room temperature for ca. 2 h. Evaporation of volatiles under reduced pressure, extraction of the residue with light petroleum (2 × 20 cm³), filtration, concentration of filtrates (to ca. 10 cm³) and cooling (−20 °C) gave yellow-brown crystals. Yield: 0.22 g, 55%. Mass spectrum (EI): *m/z*, 495 [*M*⁺ − (mes)N₃]. NMR (C₆D₆): ¹H, δ 7.5 and 6.8 (s, 2 H each, aromatic), 4.8–4.5 [doublet of doublets, 4 H, η^6 -C₆H₄(Me)Pr¹], 2.3 (s, 3 H, *p*-MeC₆H₂Me₂), 2.1 (s, 6 H, *o*-Me₂C₆H₂Me), 2.0 [spt, 1 H, η^6 -C₆H₄(Me)CHMe₂], 1.5 (s, 9 H, *p*-Bu¹C₆H₂Bu¹₂), 1.4 (s, 3 H, η^6 -MeC₆H₄Pr¹), 1.3 (s, 18 H, *o*-Bu¹₂C₆H₂Bu¹) and 0.7 [d, 6 H, η^6 -C₆H₄Me(CHMe₂)].

X-Ray crystallography

X-Ray data for all of the compounds were collected at 150 K. A FAST TV area detector diffractometer with Mo-K α radiation ($\lambda = 0.710 69 \text{ \AA}$) was employed, as previously described.¹³ The structures of compounds **2**, **6** and **8** were solved using the PATT instruction of SHELXS 86,¹⁴ whilst those of the carbodiimide and **3**, **4b**, **5** and **9** were solved *via* direct methods procedures of the same program. They were refined by full-matrix least squares on F_o^2 , using the program SHELXL 93.¹⁵ All data used were corrected for Lorentz-polarization factors, and subsequently for absorption using the program DIFABS¹⁶ with maximum and minimum correction factors listed in Table 10. The non-hydrogen atoms of the carbodiimide and compounds **2**, **4b** and **6** were refined with anisotropic thermal parameters. Compounds **3** and **5** exhibited fragile crystals of platy morphology which gave rise to poor-quality data, therefore only the heavy atoms of these structures were anisotropically refined. The non-hydrogen atoms of **8** and **9** were refined with anisotropic thermal parameters, except for the carbon atoms of the highly disordered solvate molecules, originating from light petroleum, and identified as pentane in both compounds. The hydrogen atoms of the solvate molecules in **8** and **9** were ignored. The phenyl hydrogen atoms of **8** and **9** were experimentally located whilst the remainder were placed in idealized positions. The phenyl and isopropyl hydrogen atoms of **4b** and **6** were experimentally located, whilst the remaining hydrogen atom positions were again calculated. All of the hydrogen atoms in the carbodiimide and compounds **2**, **3** and **5**

were included in idealized positions. Compounds **2** and **3** exhibit large residual peaks in the difference map which lie in the vicinity of the metal atoms. This arises from poor-quality data in the latter case, and due to a slight twinned component in crystals of the former. The equations used in the refinement, the weighting scheme and parameters employed for each compound are included as a footnote to Table 10.

Atomic coordinates, thermal parameters and bond lengths and angles have been deposited at the Cambridge Crystallographic Data Centre (CCDC). See Instructions for Authors, *J. Chem. Soc., Dalton Trans.*, 1996, Issue 1. Any request to the CCDC for this material should quote the full literature citation and the reference number 186/186.

Acknowledgements

We thank the EPSRC for support (to A. A. D.) and provision of X-ray facilities. We are indebted to Johnson Matthey plc for loan of platinum group metals and to Professor W. B. Motherwell for discussions.

References

- 1 A. A. Danopoulos, G. Wilkinson, T. K. N. Sweet and M. B. Hursthouse, *J. Chem. Soc., Dalton Trans.*, 1996, 271.
- 2 (a) D. S. Glueck, J. Wu, F. J. Hollander and R. G. Bergman, *J. Am. Chem. Soc.*, 1991, **113**, 2041; (b) D. A. Dobbs and R. G. Bergman, *Organometallics*, 1994, **13**, 4594.
- 3 A. K. Burrell and A. J. Steedman, *J. Chem. Soc., Chem. Commun.*, 1995, 2109.
- 4 (a) R. R. Savers, *Tetrahedron Lett.*, 1996, **37**, 149; A. J. Arduengo, III, J. R. Goerlich and W. J. Marshall, *J. Am. Chem. Soc.*, 1995, **117**, 11027; A. J. Arduengo, III, S. F. Gamper, M. Tamm, J. C. Calabrese, F. Davidson and H. A. Graig, *J. Am. Chem. Soc.*, 1995, **117**, 572; (b) A. J. Arduengo, III, S. F. Gamper, J. C. Calabrese and F. Davidson, *J. Am. Chem. Soc.*, 1994, **116**, 4391; (c) A. J. Arduengo, III, M. Tamm, S. J. McLain, J. C. Calabrese, F. Davidson and W. J. Marshall, *J. Am. Chem. Soc.*, 1994, **116**, 7929; H. Schumann, M. Glanz, J. Writerfield, H. Hemling, N. Kuhn and T. Kratz, *Chem. Ber.*, 1994, **127**, 2369; (d) W. A. Herrmann, M. Elison, J. Fischer, C. Köcher and G. R. Artus, *Angew. Chem., Int. Ed. Engl.*, 1995, **34**, 2371.
- 5 H.-W. Lam, G. Wilkinson, B. Hussain-Bates and M. B. Hursthouse, *J. Chem. Soc., Dalton Trans.*, 1993, 781.
- 6 R. I. Michelman, R. G. Bergman and R. A. Andersen, *Organometallics*, 1993, **12**, 2741.
- 7 W. C. Trogler, *Acc. Chem. Res.*, 1990, **23**, 426; S. W. Lee and W. C. Trogler, *Inorg. Chem.*, 1990, **29**, 1659; K. E. Meyer, P. J. Walsh and R. G. Bergmann, *J. Am. Chem. Soc.*, 1995, **117**, 974.
- 8 C. White, A. Yates and P. M. Maitlis, *Inorg. Synth.*, 1992, **29**, 229.
- 9 (a) C. H. Winter, S. Pirzad, D. D. Graf, D. H. Ceo and M. J. Heeg, *Inorg. Chem.*, 1993, **32**, 3654; (b) S. May, P. Reinsalu and J. Powell, *Inorg. Chem.*, 1980, **19**, 1582; (c) W. D. Jones and F. J. Feher, *Inorg. Chem.*, 1984, **23**, 2376; (d) P. J. Stang, Y.-H. Huang and A. M. Aref, *Organometallics*, 1992, **11**, 231.
- 10 A. A. Danopoulos, A. C. C. Wong, G. Wilkinson, B. Hussain-Bates and M. B. Hursthouse, *J. Chem. Soc., Dalton Trans.*, 1990, 315.
- 11 A.-G. Farbenfabriken Bayer, Fr. Demande, 2 000 746, 1969; *Chem. Abstr.*, 1970, **72**, 111 012m.
- 12 K. Baum, *J. Org. Chem.*, 1968, **33**, 4333.
- 13 A. A. Danopoulos, G. Wilkinson, B. Hussain-Bates and M. B. Hursthouse, *J. Chem. Soc., Dalton Trans.*, 1991, 1855.
- 14 G. M. Sheldrick, SHELXS 86, *Acta Crystallogr., Sect. A*, 1990, **46**, 467.
- 15 G. M. Sheldrick, SHELXL 93, Program for Crystal Structure Refinement, University of Göttingen, 1993.
- 16 N. P. C. Walker and D. Stuart, *Acta Crystallogr., Sect. A*, 1983, **39**, 158 (adapted for FAST geometry by A. Karaulov, University of Wales, Cardiff, 1991).

Received 18th March 1996; Paper 6/01850E